# Supplementary Information

# Monitoring the Macrophage Response to Biomaterial Implants Ex vivo Using Raman Microspectroscopy

Chuan-en Lu[1], Ruth E Levey[2], Giulio Ghersi[3,4], Nathan Schueller[1], Simone Liebscher[1], Shannon L Layland[1], Katja Schenke-Layland[1, 5, 6], Garry P Duffy[2 ,7], Julia Marzi[1, 5, 6*]

| Raman shifts ($cm^{-1}$) | Biological assignment |
|---|---|
| 1651 | Amide I[1] |
| 1623 | Tryptophan[2] |
| 1611 | Tyrosine[3] |
| 1579 | Pyrimidine ring[4] |
| 1488 | Guanine (N7)[5] |
| 1448 | Collagen[6] |
| 1379 | $CH_3$[4] |
| 1342 | Guanine[7] |
| 1330 | DNA and phospholipids[8, 9] |
| 1321 | Amide III (α-helix)[10] |
| 1309 | $CH_3/CH_2$ twisting[11] |
| 1114 | $NH_3$[12] |
| 1043 | Proline[13] |
| 1004 | Phenylalanine[11] |
| 972 | C-C backbone[13] |
| 923 | C-C backbone[13] |
| 879 | Tryptophan, Hydroxyproline[11] |
| 857 | Tyrosine, hydroxyproline[11, 14] |
| 856 | Proline, hydroxyproline[11] |
| 815 | Proline, hydroxyproline[11] |
| 786 | 5-Methylcytosine[15, 16] |
| 725 | Adenine[17] |

**Supplementary Table 1: Biological assignments of relevant Raman peaks.**

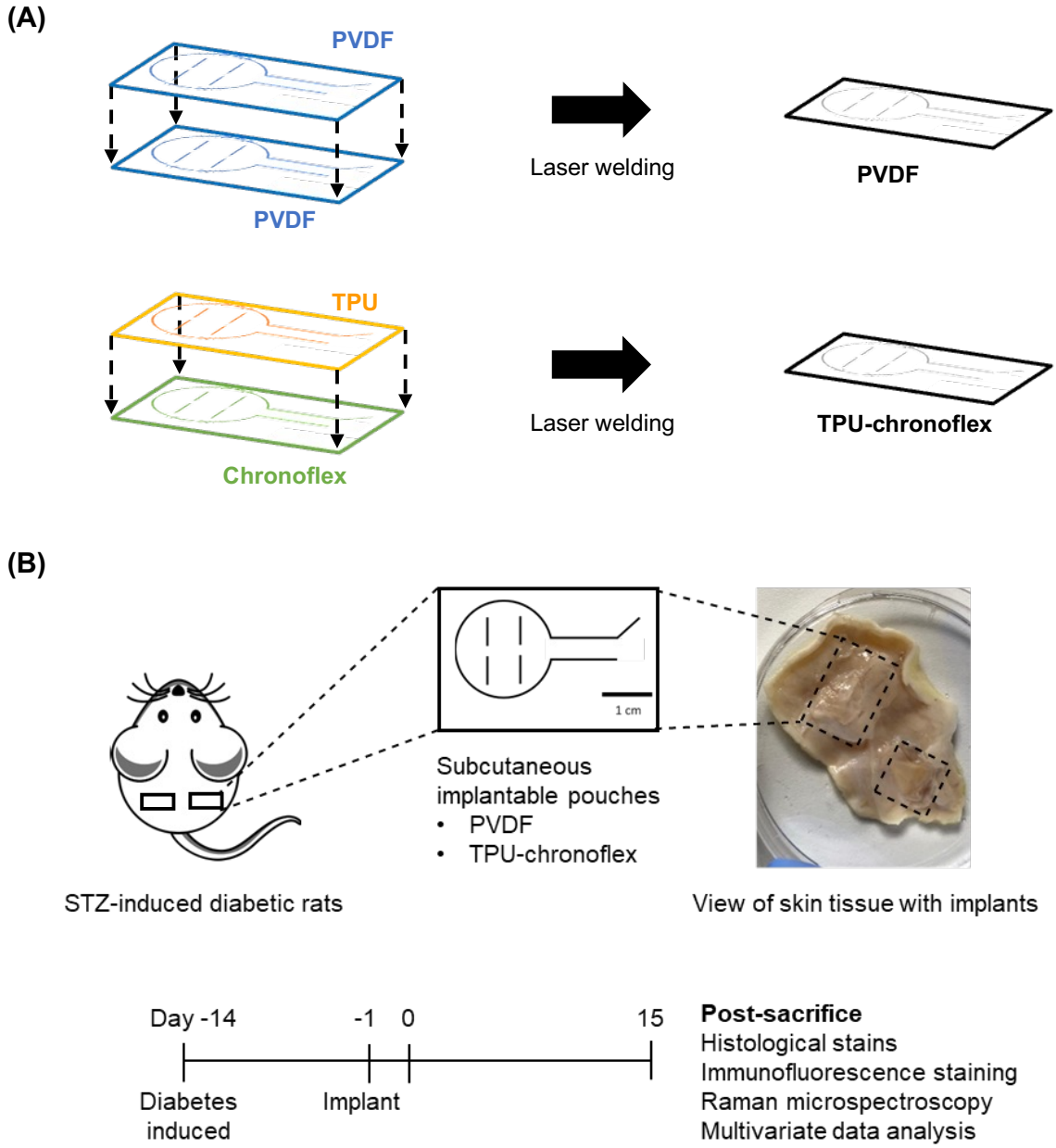


**Supplementary figure 1. Implantable pouches and scheme of study design. (A)** Fabricated sheets, PVDF and TPU-chronoflex with 50 µm thickness and 2 µm pore size, generated by laser-welding method. **(B)** Diabetes was induced by utilizing STZ 14 days before implantation. PVDF and TPU-chronoflex pouches were implanted subcutaneously at the back of the diabetic rats over 15 days.

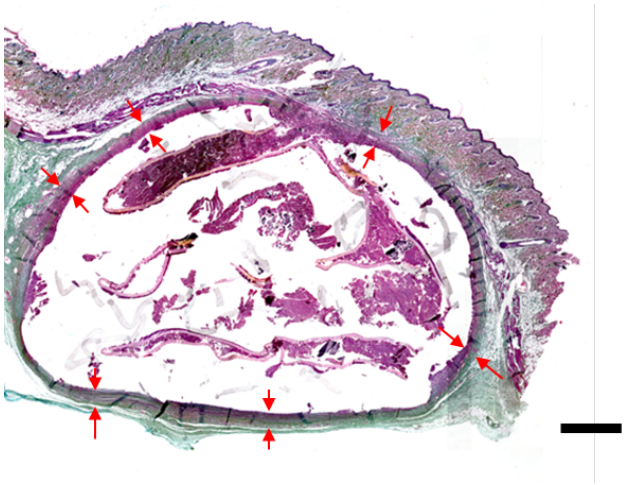

**Supplementary figure 2. Depiction of capsular thickness measurement from three regions of fibrotic capsule at the upper layer of the implant and 3 sections from the bottom.** scale bar equals 1 mm.

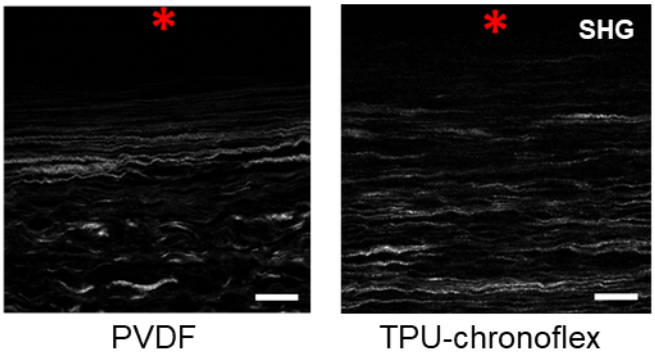


**Supplementary figure 3. Second harmonic generation (SHG) signals of Collagens in PVDF and TPU-chronoflex groups.** Red asterisk: implant side. Scale bars = 20 µm.

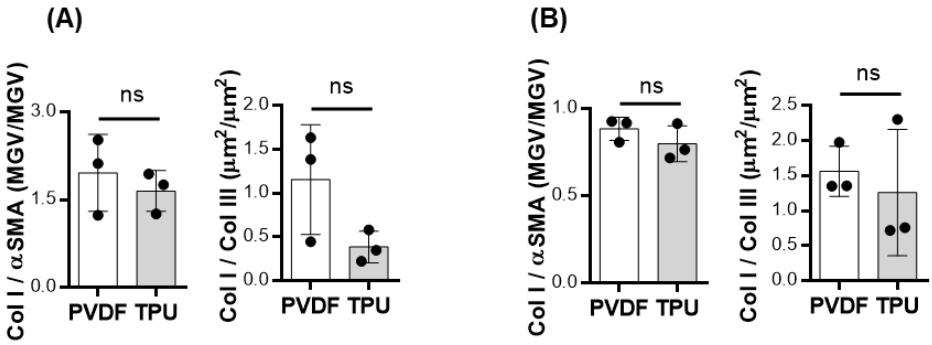


**Supplementary figure 4. Ratio Quantification of Col I, Col III and αSMA in the fibrotic capsule**. (A) IF imaging (B) Raman imaging. N=3, t test, p* ≤ 0.05.

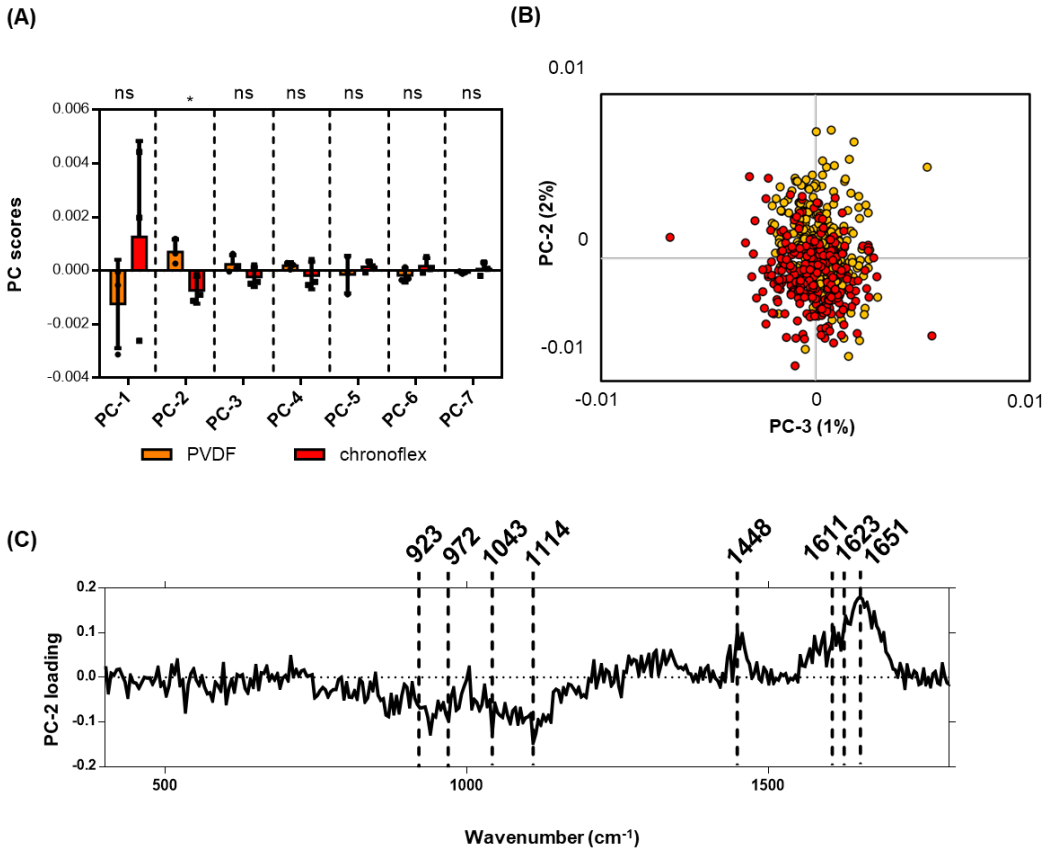


**Supplementary Figure 5. Multivariate analysis discriminates Col I composition in PVDF and TPU-chronoflex samples. (A)** Average PC-score values of Col I spectra indicate significant difference of fibrotic tissues between two implants in PC-2. n=3, p*< 0.05. **(B)** PC-2 vs PC-3 scores plot shows a separation in fibrotic capsule Col I features between PVDF and TPU-chronoflex. **(C)** PC-2 loadings identifies relevant spectral changes in Col I spectra.

## References

[1] P.J. Caspers, H.A. Bruining, G.J. Puppels, G.W. Lucassen, E.A. Carter, In Vivo Confocal Raman Microspectroscopy of the Skin: Noninvasive Determination of Molecular Concentration Profiles, Journal of Investigative Dermatology 116(3) (2001) 434-442.
[2] N. Huang, M. Short, J. Zhao, H. Wang, H. Lui, M. Korbelik, H. Zeng, Full range characterization of the Raman spectra of organs in a murine model, Opt Express 19(23) (2011) 22892-909.
[3] H. Abramczyk, A. Imiela, B. Brożek-Płuska, M. Kopeć, J. Surmacki, A. Śliwińska, Aberrant Protein Phosphorylation in Cancer by Using Raman Biomarkers, Cancers 11(12) (2019) 2017.
[4] N. Stone, C. Kendall, J. Smith, P. Crow, H. Barr, Raman spectroscopy for identification of epithelial cancers, Faraday Discuss 126 (2004) 141-57; discussion 169-83.
[5] A. Ruiz-Chica, M. Medina, F. Sánchez-Jiménez, F. Ramírez, Characterization by Raman spectroscopy of conformational changes on guanine–cytosine and adenine–thymine oligonucleotides induced by aminooxy analogues of spermidine, Journal of Raman Spectroscopy 35 (2004) 93-100.
[6] S. Kaminaka, H. Yamazaki, T. Ito, E. Kohda, H.-o. Hamaguchi, Near-infrared Raman spectroscopy of human lung tissues: possibility of molecular-level cancer diagnosis, Journal of Raman Spectroscopy 32(2) (2001) 139-141.
[7] Z. Liu, C. Davis, W. Cai, L. He, X. Chen, H. Dai, Circulation and long-term fate of functionalized, biocompatible single-walled carbon nanotubes in mice probed by Raman spectroscopy, Proceedings of the National Academy of Sciences 105(5) (2008) 1410-1415.

[8] U. Utzinger, D.L. Heintzelman, A. Mahadevan-Jansen, A. Malpica, M. Follen, R. Richards-Kortum, Near-Infrared Raman Spectroscopy for in Vivo Detection of Cervical Precancers, Appl. Spectrosc. 55(8) (2001) 955-959.
[9] R. Malini, K. Venkatakrishna, J. Kurien, K.M. Pai, L. Rao, V.B. Kartha, C.M. Krishna, Discrimination of normal, inflammatory, premalignant, and malignant oral tissue: a Raman spectroscopy study, Biopolymers 81(3) (2006) 179-93.
[10] R. Jyothi Lakshmi, V.B. Kartha, C. Murali Krishna, R.S. JG, G. Ullas, P. Uma Devi, Tissue Raman spectroscopy for the study of radiation damage: brain irradiation of mice, Radiat Res 157(2) (2002) 175-82.
[11] W.T. Cheng, M.T. Liu, H.N. Liu, S.Y. Lin, Micro-Raman spectroscopy used to identify and grade human skin pilomatrixoma, Microsc Res Tech 68(2) (2005) 75-9.
[12] K.I. Hadjiivanov, D.A. Panayotov, M.Y. Mihaylov, E.Z. Ivanova, K.K. Chakarova, S.M. Andonova, N.L. Drenchev, Power of Infrared and Raman Spectroscopies to Characterize Metal-Organic Frameworks and Investigate Their Interaction with Guest Molecules, Chemical Reviews 121(3) (2021) 1286-1424.
[13] F. Bonnier, H.J. Byrne, Understanding the molecular information contained in principal component analysis of vibrational spectra of biological systems, Analyst 137(2) (2012) 322-32.
[14] C.A. Lieber, H.E. Nethercott, M.H. Kabeer, Cancer field effects in normal tissues revealed by Raman spectroscopy, Biomed. Opt. Express 1(3) (2010) 975-982.
[15] R. Daum, E.M. Brauchle, D.A.C. Berrio, T.P. Jurkowski, K. Schenke-Layland, Non-invasive detection of DNA methylation states in carcinoma and pluripotent stem cells using Raman microspectroscopy and imaging, Scientific Reports 9(1) (2019) 7014.
[16] A. Barhoumi, N.J. Halas, Detecting Chemically Modified DNA Bases Using Surface-Enhanced Raman Spectroscopy, The Journal of Physical Chemistry Letters 2(24) (2011) 3118-3123.
[17] J.W. Chan, D.S. Taylor, T. Zwerdling, S.M. Lane, K. Ihara, T. Huser, Micro-Raman spectroscopy detects individual neoplastic and normal hematopoietic cells, Biophys J 90(2) (2006) 648-56.